http://dx.doi.org/10.12785/ugric/2025014

MULTI-OBJECTIVE DESIGN OPTIMIZATION OF A CORONARY STENT

Abbas Fadhel Abbas Zbayel
Mechanical Engineering Department
University of Bahrain
Manama, Bahrain
abbas.zbayel@gmail.com

Ali Ahmed Madan Mohammed
Mechanical Engineering Department
University of Bahrain
Manama, Bahrain
alimadan.226@gmail.com

Sayed Ali Ahmed Alawi Almosawi
Mechanical Engineering Department
University of Bahrain
Manama, Bahrain
s.aalmosawii@gmail.com

Dr. Raguraman Kannan
Mechanical Engineering Department
University of Bahrain
Manama, Bahrain
rkannan@uob.edu.bh

***Abstract*— This project focused on the design, simulation, and optimization of a coronary stent tailored for treating coronary artery diseases while meeting clinical requirements. A balloon-expandable, open-cell stent design was developed using 316L stainless steel, offering a balance between flexibility and radial strength. Advanced simulation tests, including expansion, radial compression, and fatigue tests, were performed to evaluate the stent's performance under physiological conditions. The optimized design achieved a radial strength of 429 MPa, ensuring sufficient support against vessel collapse, and a fatigue usage factor of 0.458, demonstrating durability under repetitive loading.**

Key performance indicators such as dogboning, foreshortening, and radial recoil were optimized within ranges consistent with clinical standards, ensuring a balance between structural integrity and adaptability. Multi-objective optimization was utilized to adjust strut width (0.07–0.09 mm) and length (1–1.8 mm), allowing for trade-offs between conflicting objectives such as strength and flexibility. The final design achieved 26.7% artery coverage when fully expanded, restoring the artery's diameter to a healthy 4 mm.

This project integrates engineering principles and medical requirements to produce high-performance stent. The outcomes highlight the potential for improving patient outcomes through meticulous design and optimization while adhering to clinical and manufacturing constraints.

Keywords—Coronary stent design, Multi-objective optimization, Machine learning, Surrogate model.

I. INTRODUCTION

A. Motivation

The motivation to undertake this project comes from a strong sense of responsibility to improve healthcare and help patients live better lives. Coronary artery disease is a major cause of death worldwide, responsible for 7.4 million deaths in 2012 [3]. Seeing these challenges inspired us to design a solution that could make a real difference. Balloon-expandable drug-eluting stents are widely used today, making up about 75% of stenting procedures in the United States [3], which further encouraged us to work on enhancing this life-saving technology.

B. Aim of the project

The aim of this project is to design a coronary stent by analyzing its structural performance and identifying the optimal geometric parameters that enhance its structural behavior through multi-objective optimization. The project seeks to achieve a design that meets clinical standards while addressing coronary artery disease effectively.

C. Constraints

We focused on sustainability by choosing safe and durable materials, ensured health and safety by following medical standards, and upheld ethics by following the standards provided in the next section.

D. Standards

In our project, we adhered to established standards to ensure the safety, health, and durability of our stent design. We followed ISO 10993 for biocompatibility, and ASTM standards such as F3067-14, F2079−09, F2081−06, and F2606−08 for mechanical performance and testing. Additionally, we referred to the FDA's 2010 guidelines for Non-Clinical Engineering Tests and Recommended Labeling for Intravascular Stents to align with industry benchmarks.

E. Report Outline

In this report, we introduce coronary stents, covering their definition, purpose, deployment procedures, and types followed by clinical requirements and Key Performance Indicators (KPIs), Also, we discuss stent geometries, including design variables and commercial models, and manufacturing processes (chapter 2). Material and Manufacturing selection, House of Quality (HOQ), Finite element simulations and Optimization are detailed in (chapter 3). Then, Discussions of the main result (chapter 4) followed by conclusions and recommendations for future research.

II. THEORETICAL BACKGROUND AND LITERATURE REVIEW

Chapter 2 provides an overview of coronary stents, explaining what they are, their clinical requirements, and the key performance indicators used to evaluate their effectiveness. It also discusses different stent geometries, and the manufacturing processes involved in their production.

A. What is coronary stent

Definition

A coronary stent is a small, tubular medical device used to treat coronary artery disease by supporting the walls of narrowed or blocked arteries and maintaining blood flow to the heart. It serves as a vascular scaffold, restoring proper lumen size and improving blood circulation in the treated artery [4].

Coronary Artery

The coronary arteries are the blood vessels responsible for delivering oxygen and nutrients to the heart muscle. They play

a crucial role in maintaining heart function by ensuring an adequate blood supply [5].

Deployment (Procedure)

The coronary stent deployment involves navigating a guidewire to the blockage, positioning a stent crimped onto a balloon catheter, inflating the balloon to expand the stent and restore blood flow (Figure 1), and then deflating and removing the balloon, leaving the stent in place.

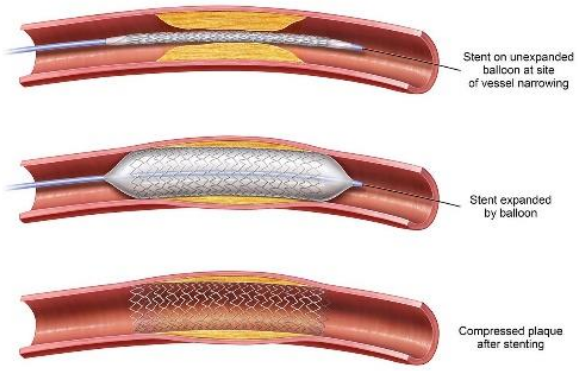

Figure 1 Deployment of the Ballon-Expandable stent [1].

In this study, we employed an open-cell stent design that is expanded using a balloon mechanism (Table 1). Additionally, the stent is a Drug-Eluting Stent (DES), which releases medication to help prevent the artery from narrowing again after deployment. These features are integral to the stent's functionality and effectiveness in treating coronary artery blockages [3].

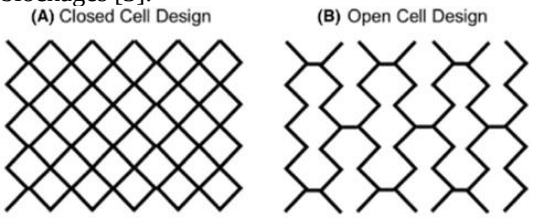

Figure 2 Closed Vs Open cell stent design

B. Clinical Requirements

The success of stenting is determined by considering both procedural and clinical factors. These factors include [4, 6]:

- Deliverability.
- Minimization of In-Stent Restenosis (ISR).
- Prevention of Stent Thrombosis (ST).
- Minimizing the risk of vessel injury.
- Stent Drug Elution.
- Maintaining artery open (Patency).
- Stent Conformability.
- Biocompatibility
- Durability

Procedural outcomes include stent deliverability, immediate increase in luminal cross-sectional area, the lack of arterial injury or immediate thrombus formation, and expansion quality of the stent. Long-term clinical success is indicated by the absence of ISR, late ST, and relevant clinical events including the requirement for repeat PCI [4].

1) Deliverability

Deliverability is a critical clinical requirement for stents, encompassing proper sizing to cross the lesion, sufficient flexibility to navigate vessels safely, and adequate visibility for accurate monitoring during procedures [6].

2) In-Stent Restenosis (ISR)

In-Stent Restenosis (ISR) refers to lumen narrowing after PCI, caused by neointimal proliferation or neo atherosclerosis in stented arteries [7]. Restenosis can occur due to excessive tissue growth or elastic artery walls tend to slowly move back after balloon angioplasty [8]. Reducing ISR requires optimizing drug coatings to inhibit cell proliferation and designing stents to enhance blood flow and minimize vessel wall stress.

3) Stent Thrombosis (ST)

Stent thrombosis (ST) is the blockage of a coronary stent by a blood clot (thrombus), potentially causing heart attack or death, with early cases linked to under expansion or malposition, and very late cases often due to neo atherosclerosis [9].

4) Vessel Injury

Vascular injury during stent placement happens due to the stent's recoil, dogboning, and pressure on the artery wall, damaging the cells lining the vessel [3, 4]. This can cause inflammation, excessive tissue growth, and complications like re-narrowing of the artery or blood clots.

Table 1 Type of stent [3].

Category	Type	Description
Based on Material	Bare-Metal Stents (BMS)	Provide structural support without drug properties.
	Drug-Eluting Stents (DES)	Coated with drugs to reduce restenosis by limiting scar tissue formation.
	Bioresorbable Stents (BRS)	Biodegradable stents that dissolve over time, leaving no permanent implant.
Based on Expansion Mechanism	Balloon-Expandable	Are mounted on a balloon in a contracted state and are deployed by inflating the balloon to expand the stent within the vessel (**Error! Reference source not found.**) expanding the stent to the desired diameter. These stents require sufficient radial strength and flexibility to adapt to the vessel shape after expansion
	Self-Expanding	are spring-like and expand to their predetermined diameter once the external constraints are removed
	Thermal Memory	lose their contracted shape when exposed to heat and regain their predetermined shape once placed in the body.
Based on Geometry	Open-cell design	Incomplete connections between adjacent struts, creating larger gaps or "cells" that enhance flexibility and adaptability to curved or tortuous vessel anatomies (**Error! Reference source not found.**).
	Closed-cell design	complete connections between adjacent struts, forming smaller and uniform cells (**Error! Reference source not found.**).

5) Stent Drug Elution

Drug-eluting stents (DES) release drugs gradually to prevent artery re-narrowing (restenosis) after stent placement by reducing smooth muscle cell growth and inflammation [6]. The drug is released from a polymer coating over time, improving healing and lowering complications for better long-term outcomes [10].

6) Patency

Patency refers to a stent's ability to stay open, ensuring unobstructed blood flow, which is essential for proper circulation in the treated artery. To achieve this, stents must provide optimal scaffolding for mechanical support to prevent vessel recoil and use biocompatible materials to maintain structural integrity and minimize adverse reactions [6].

7) Stent Conformability

Stent conformability refers to the ability of a stent to adapt to the vessel's shape, reducing vessel distortion and trauma. It depends on flexible, strong materials and advanced designs like thin struts for effective support [11].

8) Biocompatibility

Biocompatibility refers to a stent's ability to function without causing harmful biological reactions. Compliance with ISO 10993 guidelines ensures the safety and compatibility of medical devices with biological systems [12].

9) Durability

Durability is a critical clinical requirement for stents, ensuring they maintain structural integrity and functionality over time under physiological conditions. Durable stents must resist fatigue, corrosion, and mechanical stress to provide long-term support without failure or degradation.

C. Key Performance Indicators (KPI)

The engineering attributes of stents play a critical role in their efficacy and safety. A meticulous evaluation of these attributes ensures that stents not only meet stringent regulatory standards but also achieve the desired clinical outcomes, providing a reliable solution for treating vascular diseases.

Assessing stent performance to meet clinical requirements involves evaluating several critical engineering attributes [4]:

- Recoil
- Bending Flexibility (Crimped)
- Stent Stresses (Structural)
- Dogboning
- Foreshortening
- Radial Strength
- Radial Stiffness
- Fatigue Resistance
- Stent Artery Coverage

Intra-deployment

Post-deployment

These Key Performance Indicators (KPIs) for a stent can indeed be classified into intra-deployment (during the procedure) and post-deployment (after the procedure) phases.

1) Radial Recoil

The reduction in the outer diameter of a stent after deflating the delivery balloon is referred to as radial recoil (RR). Minimal stent recoil is crucial as it prevents the need for excessive expansion to achieve the desired final diameter, thereby reducing the risk of tissue damage and arterial injury [13]. Factors influencing recoil include the stent's material properties and geometric design (Figure 3). The recoil percentage is determined using the formula:

$$Stent\ Recoil\ (\%) = \left(1 - \frac{D_{final}}{D_{inflated}}\right) * 100 \qquad (1)$$

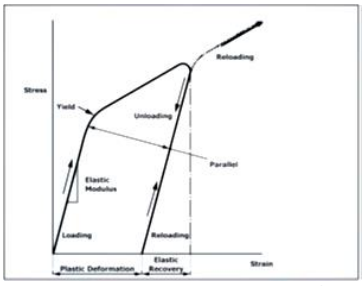

Figure 3 Elastic recovery is responsible for recoil.

Here, $D_{inflated}$ refers to the stent's outer diameter when the balloon is fully inflated, and D_{final} is its diameter after deflation [14].

2) Bending Flexibility

To reach the targeted site, a stent must navigate through tight vascular passages, requiring high flexibility in its unexpanded, crimped state. Flexibility can be quantified using the moment-curvature curve from bending simulations (Figure 4), which considers the moment created by bending deformation and curvature

$$\kappa = \frac{\frac{\partial^2 y}{\partial z^2} + \frac{\partial^2 z}{\partial x^2}}{[1 + (\frac{\partial y}{\partial z})^2 + (\frac{\partial z}{\partial x})^2]^{\frac{3}{2}}} \qquad (2)$$

The bending resistance is the area under the moment-curvature curve (Figure 5), indicating how much force is needed to achieve a certain curvature:

$$Bending\ Resistance = \int_0^{\kappa_d} M(\kappa)\, d\kappa \qquad (3)$$

Where M is the moment force, bending resistance is determined by the area under the moment-curvature curve in the linear region to prevent plastic deformation [13, 15].

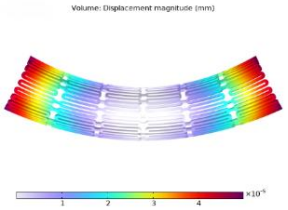

Figure 4 Bending test simulations.

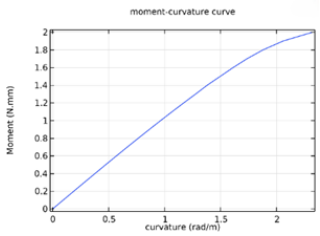

Figure 5 Moment-curvature curve.

3) Stent Stress

The stress on the stent during deployment, measured by taking the maximum stress (Figure 6) within the stent geometry [13].

$$stent\ stress = \max(stress\ in\ geometry) \qquad (4)$$

Residual stress in an artery stent is important because it represents the stress remaining in the stent material after deployment, due to plastic deformation during crimping and expansion. To calculate residual stress, a similar approach

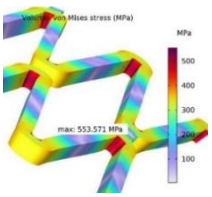

Figure 6 Stress Distribution.

can be used for stent stress in the state of post-deployment, accounting for any recoil effects.

4) Dogboning

The non-uniform expansion of a coronary stent during deployment leads to a shape resembling a "dogbone," where the central part is narrower than the ends [4]. The Dogboning Ratio (Figure 7) quantifies this effect by measuring the difference between the maximum diameter at the distal ends $D_{max,end}$ and the minimum diameter at the central part $D_{min,central}$, expressed as a percentage [16]:

$$Dogboning = \frac{D_{max,end} - D_{min,central}}{D_{max,end}} \cdot 100\ (\%) \qquad (5)$$

A higher ratio indicates more non-uniform expansion, potentially affecting the stent's fit with the artery wall (Figure 8).

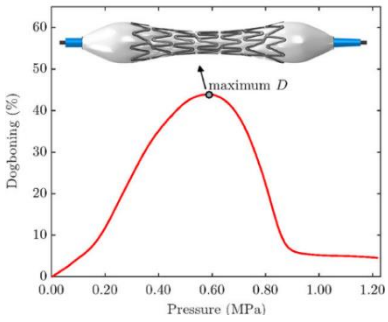

Figure 7 Dogboning profile during loading phase of deployment

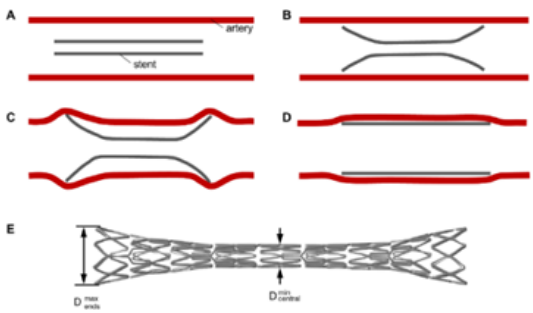

Figure 8 Crimped stent in artery. B: Stent begins to expand. C: Artery overstretching due to dogboning. D: Final stent configuration inside the artery. E: Dogboning effect.

5) Foreshortening (FS)

Axial shortening occurs when a stent expands, causing a reduction in its length from the crimped state L_0 to the expanded state L_{final} [17]. This change is expressed as a percentage and can impact the accurate placement of the stent, potentially preventing it from fully covering plaque (Figure 9). The formula for calculating this change is:

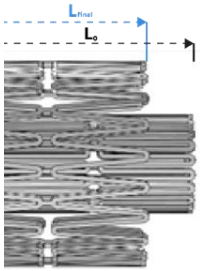

Figure 9 Foreshortening (FS).

$$FS = \frac{L_0 - L_{final}}{L_0} \cdot 100 \qquad (6)$$

6) Radial strength

The maximum radial loads a stent can withstand before plastic deformation [3], as defined by ASTM F3067-14, is determined through testing the stent's radial force against its radial deformation. The force-displacement curve is normalized by stent length, and the peak value represents the maximum radial force before plastic deformation

$$Radial\ strength(RS) = \max(radial\ force) \qquad (7)$$

7) Radial Stiffness

The ability of a stent to resist radial deformation when exposed to external forces is crucial for maintaining vessel support and diameter. This property is quantified by the force required to produce a specific amount of radial deflection. Radial stiffness is calculated from the slope of the radial deformation vs. radial force curve (Figure 10) in its linear region, reflecting the stent's resistance to deformation [4].

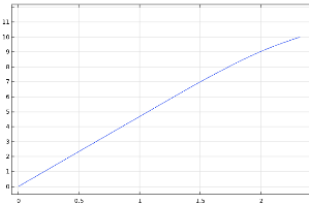

Figure 10 Radial deformation vs. radial force curve.

8) Artery coverage

The proportion of an artery's circumference covered by a stent's struts is calculated as:

$$Stent\ artery\ coverage = \frac{A_{stent}}{A_0} \cdot 100 \qquad (8)$$

Where A_{stent} is the external surface area of the stent and A_0 is the internal surface area of the artery covered by the stent. This coverage is essential for providing artery support and preventing restenosis [4].

9) Fatigue

Fatigue refers to the weakening or failure of an artery stent due to repetitive cyclic loading, such as blood flow pressure changes and the bending of the artery. This process involves the accumulation of small, repetitive deformations that can lead to cracks or fractures over time, potentially causing the stent to lose structural integrity and functionality within the artery. The load cycle can be computed using a sequence of stationary loads, enabling evaluations such as stress-based and stress-life assessments (Table 2) [18].

Table 2 Comparison of Stress-Based and Stress-Life Fatigue Approaches.

	Stress-Based	Stress-life
Purpose	Assess proximity to fatigue limit (safety evaluation)	Predict number of cycles to failure (lifespan).
Result	Fatigue Usage Factor (f_{us})	Number of cycles to failure (N)
Applicability	High-cycle fatigue with elastic behavior	High-cycle fatigue with empirical data
Criterion	Findley, Matake, Normal stress	S-N curve

Findley Criterion

Considers the maximum shear stress amplitude and the effect of a normal stress component on a critical plane. To analyze fatigue behavior under sinusoidal fluctuating stress (Figure 11), the stress ratio R is defined as R=$\sigma_{min}/\sigma_{max}$, with the maximum stress expressed as $\sigma_{max} = \frac{2\sigma_a}{1-R}$. The fatigue failure equation is given as:

$$\sqrt{{\sigma_a}^2 + (k\sigma_{max})^2} + k\sigma_{max} = 2f \qquad (9)$$

Here, k and f are material parameters. The critical plane is the one that maximizes the left-hand side of the equation. To determine k and f, two fatigue tests under different loading conditions (e.g., using two different stress ratios R) are required.

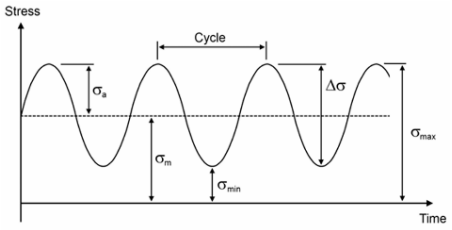

Figure 11 Sinusoidal fluctuating stress.

The fatigue usage factor f_{us} , is the ratio between the left-hand side of the Findley criterion and the right-hand side, that measures the ratio of a material's accumulated fatigue damage to its total fatigue life. A value below 1 means that the component is loaded below the fatigue limit [19].

$$f_{us} = \frac{\sqrt{{\sigma_a}^2 + (k\sigma_{max})^2} + k\sigma_{max}}{2f} \quad (10)$$

Matake Criterion

Like the Findley criterion but emphasizes the maximum normal stress on the critical plane. The difference is that it is the plane with maximum shear stress range that is taken as the critical plane, and the maximum normal stress is evaluated on that plane. The expression is:

$$\frac{\sigma_a}{2}\left(1 + \frac{k\sigma_{max}}{\sigma_a}\right) = f \quad (11)$$

Here, k and f are material parameters. The critical plane is the one that maximizes the left-hand side of the equation. The same approach of Findlay is used to determine k and f [19]. Note that k and f are different for each Criterion and the fatigue usage factor for normal stress is defined

$$f_{us} = \frac{\frac{\sigma_a}{2}\left(1 + \frac{k\,\sigma_{max}}{\sigma_a}\right)}{f} \quad (12)$$

Normal Stress Criterion

Evaluates the fatigue limit directly using the maximum normal stress. The contribution from the shear stress is ignored and the plane which experiences the maximum normal stress range, $\Delta\sigma_a$, is considered as the critical plane. The criterion is defined with the following expression

$$2\sigma_a = f \quad (13)$$

The fatigue usage factor for normal stress is defined

$$f_{us} = \frac{2\sigma_a}{f} \quad (14)$$

S-N curve

also known as the Wohler curve (Figure 12), represents the relationship between stress amplitude (σ_a) and the number of cycles to failure (N) under constant stress cycling. It is expressed as:

$$\sigma_a = f_{SN}(N) \quad (15)$$

where f_{SN} denotes the S-N function

At low stress levels, fatigue life is limited by a cycle cutoff, which for a stent is 10^7 cycles, beyond which failure does not occur. If the computed stress amplitude exceeds the highest value defined by the S-N curve, fatigue life cannot be determined, and no results are provided in such regions [18].

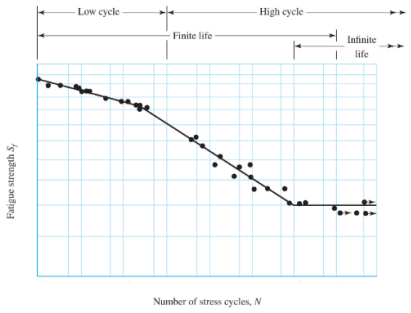

Figure 12 Wohler curve (S-N curve) [2].

D. Stent Geometries

The geometric design variables of a stent play a critical role in its mechanical performance and overall effectiveness. These variables include the strut width, strut thickness, length of the unit stent, cell shape, and crown radius (Figure 14). Each of these parameters affect key properties such as radial strength, flexibility, fatigue resistance, and arterial coverage. Optimizing these variables ensures that the stent can withstand physiological loads, minimize restenosis, and maintain effective blood flow. Additionally, the arrangement and pattern of the cells contribute to the overall stability and expansion behavior of the stent. These geometric parameters form the foundation of stent design, balancing strength, flexibility, and compatibility with the arterial wall [4].

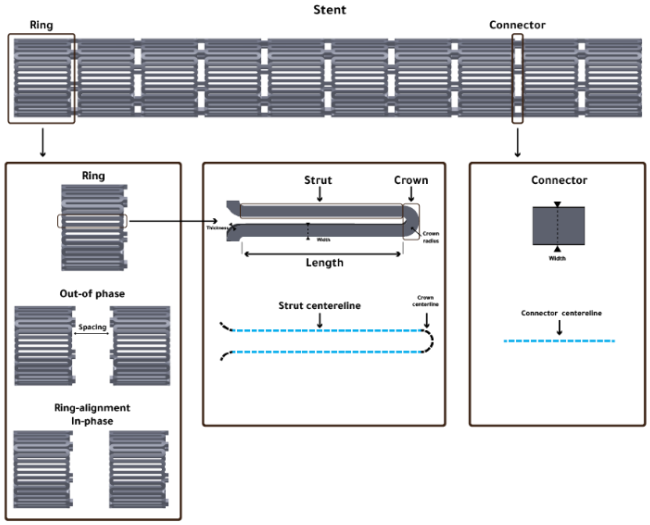

Figure 13 General parametrization scheme for geometric design variables in stent design optimization.

Here, we present a selection of commercial stent designs that share similarities with our model (Figure 13) Designs such as Xience, Onyx, Synergy, Orsiro, Elunir, and Slender illustrate the diversity of geometries and patterns utilized in stent manufacturing. By showcasing these examples, we aim to provide a clear perspective on how geometric variations influence stent performance and demonstrate how our design aligns with these established models [4].

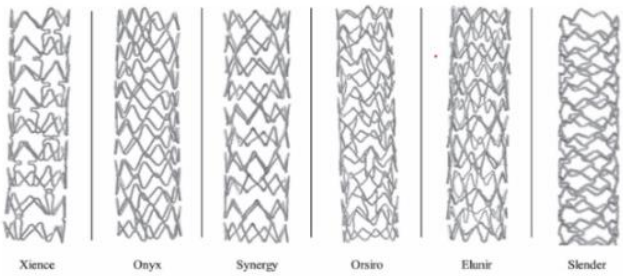

Figure 14 Stent design of six commercially available contemporary.

E. Manufacturing

1) Manufacturing Techniques

a) Braiding Technique

The technique involves winding one or more wires around a carrier and braiding them along a defined axis of rotation to create a mesh-like stent structure. This process typically uses a metal mandrel to shape the stent. The resulting structure features crossing wires that do not interlock, forming a "finger catcher" design [20]. (Figure 15).

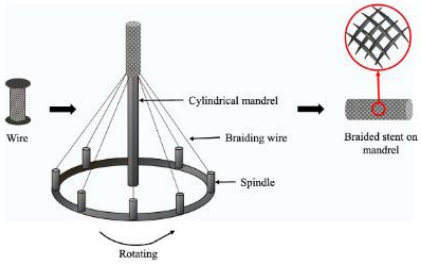

Figure 15 A Series of Connected QFD Houses.

b) Micro-Injection Molding

Micro-injection molding is a forming process where heated and melted polymer is injected into a mold to shape the material, solidifying upon cooling [21].

c) Laser Cutting

Laser cutting is a precise and commonly used manufacturing process for vascular stents. This technique utilizes a high-energy laser beam to focus on a tubular material, such as metal or polymer, causing localized heating that leads to melting, vaporization, or ablation of the material. The removed material is then blown away by high-velocity airflow, leaving behind the desired intricate structural patterns required for the stent [21]. (Figure 16).

d) 3D printing

3D printing, also known as additive manufacturing (AM), is a process that creates physical objects from digital models by adding material layer by layer. This technique offers flexibility in design, supports various materials, and enables personalized structures, making it highly valuable for medical applications, including stent manufacturing [20]. (Figure 17).

Figure 16 Laser Cutting process of stent.

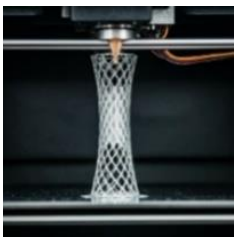

Figure 17 3D printing process of stent.

2) Choosing process

For the manufacturing of a stainless-steel artery stent with a structure consisting of sinusoidal rings alternately connected by phase-shifted links, laser cutting is the ideal choice. This process offers exceptional precision and accuracy, enabling the production of intricate and complex stent designs while maintaining uniformity across the structure. Laser cutting is highly compatible with stainless-steel, ensuring clean cuts without introducing undesired material defects. Additionally, it is a fast and efficient method, offering the potential for both small-scale customization and high-volume production. Its ability to produce sharp, detailed patterns aligns perfectly with the stent's unique design requirements, providing a reliable and high-quality manufacturing solution [21].

III. Design and Implementation

Chapter 3 focuses on the development process of our stent design. It includes HOQ analysis, material selection, detailed geometry and dimensions of the stent, finite element simulations, optimization of design parameters, and cost analysis.

A. HOQ

The House of Quality (HOQ), a key tool in Quality Function Deployment (QFD), translates customer requirements into actionable design or engineering objectives to ensure the final product or service aligns with customer expectations and organizational goals. It systematically identifies and prioritizes customer needs, clarifying what customers value most. Additionally, it analyzes the relationships between customer requirements and technical specifications to identify and address potential trade-offs, ensuring balanced and optimized solutions [22].

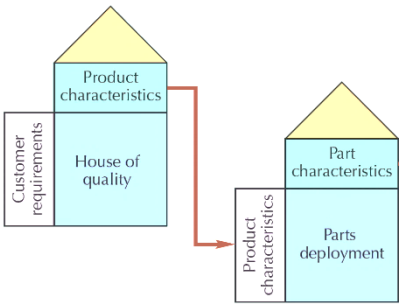

Figure 18 A Series of Connected QFD Houses.

Our design incorporates a series of two Quality Function Deployment (QFD) matrices to effectively connect customer requirements, design characteristics, and parts specifications (Figure 18). The detailed QFD's are presented in (Figure 19). The design characteristic scores were evaluated using Minitab® and will serve as inputs for the optimization process.

B. Material Selection

M. F. Ashby introduced a systematic approach to material selection using materials selection charts [2, 23], which has been applied in this report through the Ansys Granta Selector® software. The process involves (Figure 20) defining material performance requirements, translating design needs into constraints and objectives, screening unsuitable materials, ranking viable candidates by performance, the final task is selection [23].

1) Requirements

The initial step in selecting a suitable stent material lays the groundwork for transforming qualitative criteria into measurable metrics. Key performance characteristics include:

- High Strength-to-Weight Ratio: To effectively support the artery without excessive bulk.
- High Fracture Toughness: It should resist breaking during expansion.
- Excellent Fatigue Resistance: The material must endure repeated stress from artery movement.

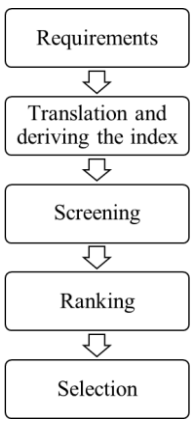

Figure 19 Material Selection Approach.

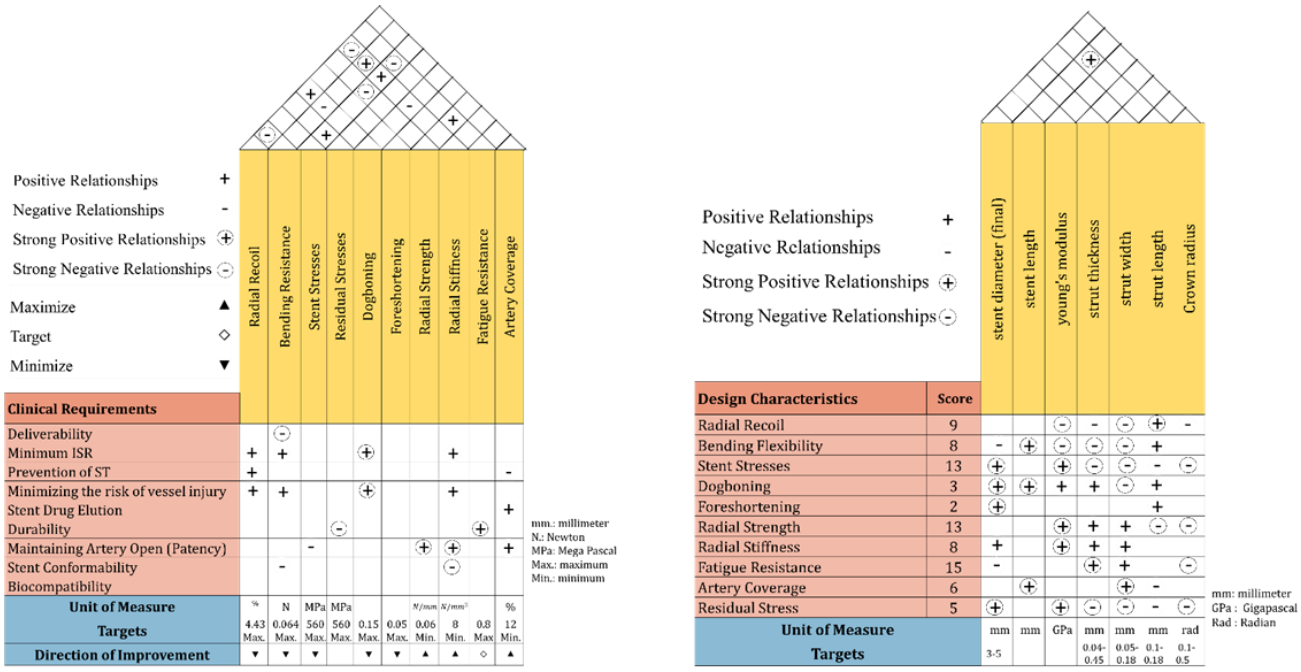

Figure 20 The detailed QFD's.

- Corrosion Resistance and Biocompatibility: It should resist corrosion and be safe for long-term implantation [12].
- High Stiffness: The material must retain its shape under load and minimize recoil.
- Cost-Effectiveness: It should balance high performance with affordability.

2) Material Indices

In this section, material indices will be derived for two load modes: bending and tension. The stent undergoes bending during and after deployment, while tension can arise from expansion, causing the stent's struts to stretch beyond their design limits, potentially leading to structural damage or failure, such as stent fractures.

The material indices for tension load are

$$M_{t1} = \frac{\rho}{E}, \qquad M_{t2} = \frac{\rho}{\sigma_y} \tag{16}$$

The material indices for bending load are

$$M_{b1} = \frac{\rho}{E^{\frac{1}{2}}}, \qquad M_{b2} = \frac{\rho}{\sigma_y^{\frac{2}{3}}} \tag{17}$$

3) Screening

Screening involves setting attribute limits to evaluate materials based on specific requirements. In stent design, critical constraints such as biocompatibility, cost, heat treatment capabilities, fatigue strength, and radiopacity ensure the stent meets functional and regulatory standards. By applying these constraints, unsuitable materials are excluded, streamlining the selection process and focusing on viable options that satisfy all design criteria.

Biocompatibility

As stents come into direct contact with patients, the material must prevent harmful biological responses. To ensure biocompatibility, we applied the ISO-10993 standard, Biological Evaluation of Medical Devices Part 1: Evaluation and Testing, as a constraint [12].

Price

A cost constraint was established to maintain market competitiveness and feasibility. The upper limit was set at $36/kg, ensuring the material balances affordability with performance and regulatory compliance. This price cap helps identify economically viable options while meeting essential design requirements.

Heat Treatment

Heat treatment significantly influences the mechanical properties of materials. Annealed metals were preferred over cold-worked materials due to their higher toughness, which enables better deformation resistance, enhancing the stent's durability.

Fatigue Strength

Fatigue failure in stents can cause severe complications, such as loss of radial support, thrombus formation, restenosis, or vessel perforation [12]. To mitigate these risks, a minimum cyclic stress threshold of 130 MPa was set, ensuring materials can endure at least 10 million cycles 10^7 without failure, thereby guaranteeing structural integrity and long-term performance.

Radiopacity

Radiopacity is essential for visualizing stents during angiographic or radiographic imaging to ensure accurate placement and allow post-procedure monitoring. The ASTM 5640-20 standard recommends a minimum radiopacity of 2 mm Al at 20 keV [24], ensuring the stent remains visible for precise positioning and ongoing evaluation.

Ashby Charts

Ashby Charts After Applying the Limits are shown in (Figure 21). The gray color indicates the materials failed to pass the Constraints.

4) Ranking

The survivor's candidate that has passed the screening step are Stainless Steel 316L, Cobalt Chromium L605, and Nickel Titanium Ni-45Ti.It is a good idea to lay out the results as a table, containing each material with its indices (Table 3).

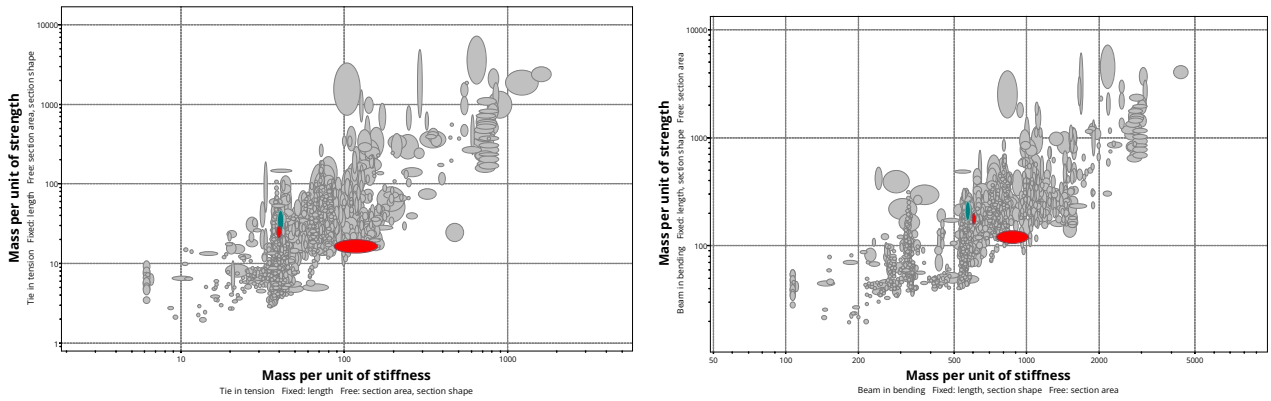

Figure 21 The tension load and bending load graphs, generated after applying the constraints, highlight the materials that meet the specified criteria, with colored markers representing the materials that successfully passed the screening process.

Table 3 Materials for Stent.

Material	Stainless Steel 316L	Cobalt Chromium L605	Nickel Titanium Ni-45Ti
$M_{t1}\left(\frac{kg/m^3}{GPa}\right)$	38.8 - 42	38.6 - 40.6	86.5 - 158
$M_{t2}\left(\frac{kg/m^3}{MPa}\right)$	25.7 - 46.9	21.4 - 29.5	13.8 - 20
$M_{b1}\left(\frac{kg/m^3}{GPa^{1/2}}\right)$	555 - 580	593 – 609	749 - 1010
$M_{b2}\left(\frac{kg/m^3}{MPa^{2/3}}\right)$	174 - 260	161 - 199	107 - 138
Comment	Higher Stiffness, lowest strength, Inexpensive	Higher Stiffness, Higher strength, Highest Fatigue Strength	Lowest Stiffness, Highest strength, Highest Toughness, Shape Memory and Super-elastic Properties, Lightest

5) Selection

Nickel Titanium, typically used for self-expanding stents due to its super elasticity (requires large deformation for plastic deformation), is excluded from consideration. Stainless Steel 316L and Cobalt Chromium exhibit similar strength and stiffness ratios; however, Stainless Steel 316L is selected due to its cost-effectiveness (7.7 USD/kg compared to 44.5 USD/kg for Cobalt Chromium) [25]. Its excellent corrosion resistance, biocompatibility (ISO-10993 [12]), and ease of manufacturing further support its selection as a practical and economical material for stent applications.

C. Geometry and Dimensions

The design of stents can be parameterized to study the influence of geometric variations on mechanical performance. This approach involves defining critical parameters, such as strut width, length, and thickness, and systematically varying them to optimize the stent's properties for its intended application.

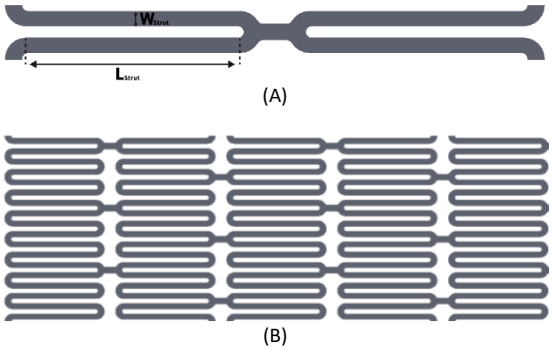

Figure 22 (A) Planar repeating unit and proposed design variables; (B) Full planar structure.

Table 4 Lower and upper limit for width and length of strut.

Design variable	Lower bound (mm)	Upper bound (mm)
w_{strut}	0.07	0.09
l_{strut}	1	1.8

In this study, we focused on optimizing two key design variables: the width and length (Figure 22) of the stent strut. The width varied between 0.07 mm and 0.09 mm (Table 4), while the length ranged from 1 mm to 1.8 mm (Table 4) To ensure consistency and isolate the effects of these variables, other geometric parameters were kept constant. These fixed parameters included the number of rings is 10, the number of struts per ring is 42, the crimped diameter of the stent is 1.915 mm, the expanded diameter is 4 mm, the strut thickness is 0.17 mm, the crown width is 0.13 mm, the connector length is 0.15 mm, and the number of connectors is 7. This approach enabled a comprehensive evaluation of the stent's mechanical behavior under different scenarios, including expansion, radial compression, and bending, providing valuable insights into optimal design configurations for enhanced performance and manufacturability.

The coronary artery consists of three main layers: the adventitia (Figure 23), which provides structural support; the media (Figure 23), composed of smooth muscle responsible for vessel contraction; and the intima (Figure 23) a thin inner layer crucial for vascular function. A healthy artery typically has an inner diameter of around 3.9 mm, while a blocked artery narrows to approximately 1.5 mm. Our stent design, when fully expanded, reaches a diameter of 4 mm, effectively restoring the artery to its healthy size by supporting the vessel walls and maintaining proper blood flow [3].

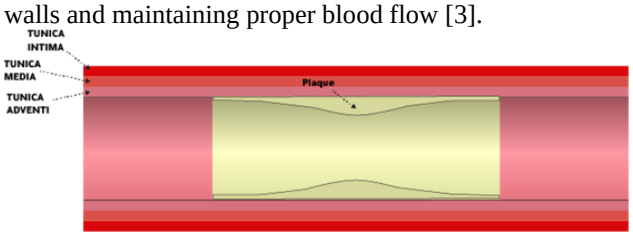

Figure 23 Geometric model of the idealized atherosclerotic coronary artery.

D. FE Simulations

COMSOL® Multiphysics is a leading software platform for finite element analysis (FEA) and Multiphysics simulation. It offers an integrated modeling environment where engineers

and researchers can simulate real-world physical phenomena. With its extensive library of predefined physics interfaces and customizable modeling capabilities.

Reasons for Choosing COMSOL® Multiphysics:

COMSOL® Multiphysics was chosen for its ability to couple multiple physics phenomena (e.g., thermal, structural, and fluid dynamics) seamlessly, making it ideal for simulating intricate stent behaviors like expansion and radial compression. Its user-friendly interface simplifies simulation workflows, while advanced meshing tools and solvers ensure high-accuracy results for small, complex geometries. Additionally, the software's customization options, versatility across various engineering applications, and extensive learning resources make it a robust tool for specialized and multidisciplinary projects [26].

1) Expansion Test (Intra-deployment)

Definition

The expansion test evaluates how a stent expands under applied radial pressure, simulating the inflation of a balloon during angioplasty. It is critical for assessing the stent's structural integrity, deformation behavior, and potential complications such as dogboning, foreshortening, and radial recoil. These parameters help ensure the stent's performance in maintaining vessel patency while minimizing arterial damage.

Methodology

a) Setting Up the Geometry

Importing geometry into **COMSOL®** Multiphysics.

- The stent design was modeled in a 3D CAD tool (**SolidWorks®** Software) and imported into **COMSOL®** 's Geometry module (Figure 24).
- To save computational resources, use a symmetric section of the stent.

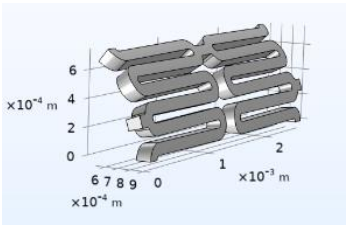

Figure 24 Importing Unit stent into COMSOL® Multiphysics interface.

b) Defining the Material

assigned material properties such as Young's Modulus, Poisson's Ratio, and Density using the Material Library in **COMSOL®**

c) Applying Boundary Conditions

1- Symmetry: Symmetry planes were defined to ensure that the deformation and loading mirrored the full stent geometry (Figure 25).

2- Plasticity: Material plasticity was applied to capture permanent deformations under high stress, using nonlinear properties of 316L stainless steel.

3- Inner Radial Pressure: A uniform inner radial pressure was gradually applied to simulate balloon inflation, replicating the expansion process realistically (Figure 25).

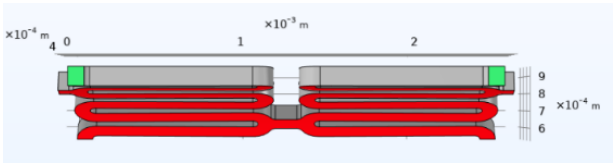

Figure 25 Applying Boundary condition. Green represents the Symmetry condition while the Red represents the Inner Radial Pressure.

d) Meshing the Geometry

Applied a controlled mesh for high accuracy and efficient computation. Triangular elements were used for the inner and outer surfaces, while rectangular elements were applied along the thickness to capture detailed deformations effectively (Figure 26).

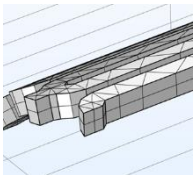

Figure 26 Controlled mesh for unit cell by using triangle and rectangle mesh.

e) Obtaining and Visualizing Results

Extracted the results, such as stress distribution, displacement, and radial expansion data (Figure 28). To visualize the complete stent design, we used mirroring and sector replication techniques in **COMSOL®** (Figure 27).

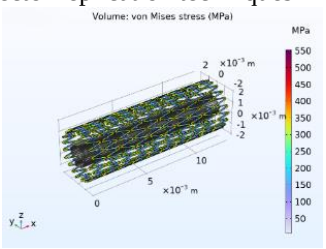

Figure 27 Multi-unit stent plot.

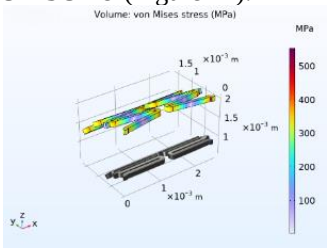

Figure 28 Single unit stent plot.

1- Dog-boning

Dog-boning is calculated by measuring the difference in expansion between the stent's center and its ends. The diameters at the center and ends are recorded, and the ratio is calculated to assess uneven expansion.

2- Foreshortening

Foreshortening is calculated by measuring the change in the stent's length before and after expansion. The difference in length is expressed as a percentage of the original length to evaluate how much the stent contracts are axially.

3- radial recoil

Radial recoil is calculated by measuring the stent's diameter immediately after balloon expansion and again after the balloon is deflated. The percentage decrease in diameter reflects the stent's tendency to return to its original shape, helping assess its structural stability and radial strength.

4- Structural stress

Structural stress is calculated by analyzing the stress distribution across the stent under applied loads, we calculate the maximum stress by focusing on the rounded shape at the end of the strut, as this region experiences stress concentration.

5- residual stress

We obtain the residual stress in the results by analyzing the stress distribution after the stent has fully expanded and the external loads are removed. Using COMSOL®, we evaluate stress values at critical points

6- artery coverage

We calculate the outer radius and length of the unit stent after expansion using **COMSOL®.** These values are then

processed in Excel to determine the stent's surface area and its artery coverage.

2) Radial Compression Test (Post-deployment)

The Radial Strength Test evaluates the stent's ability to resist external compression forces after expansion. Using **COMSOL®** Multiphysics, we applied uniform outer pressure to the expanded stent model and measured its radial strength and stiffness.

a) Preparation of Expanded Stent Model:

Performed the Expansion Test on the stent to achieve its expanded geometry, which was then directly imported into the Radial Strength simulation file in **COMSOL®**.

b) Boundary Conditions:

Uniform external pressure was applied to the outer surface of the stent to simulate physiological compression forces, and symmetrical conditions were utilized to reduce computation time while maintaining accuracy (Figure 29).

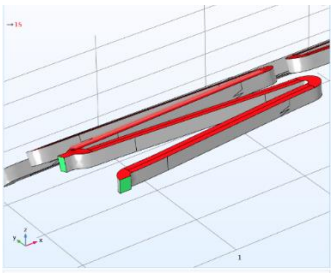

Figure 29 Boundary condition for Radial strength test. Red represents the Compression pressure and the green color represent the symmetry condition.

c) Meshing:

A high-accuracy mesh was generated with finer control, especially around critical regions like curved and thin sections, to ensure precise results.

d) Simulation and Results:

To visualize the results, we applied similar techniques used in the Expansion Test. This included mirroring and sectoring the stent geometry to generate a complete model (Figure 30).

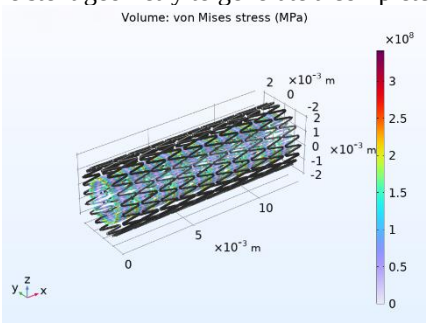

Figure 30 Stress distribution along the stent.

1- radial strength

To evaluate radial strength, we first obtained the pressure corresponding to the first non-zero plastic strain by measuring the equivalent plastic strain at the crowns of the stent in **COMSOL®.** The radial strength was then calculated by multiplying this pressure by the area of the unit stent and dividing it by the length of the unit stent.

2- radial stiffness

To evaluate the radial stiffness, we determined the slope of the radial deformation versus applied pressure curve. The pressure values were taken from zero up to the point where the stent began to plastically deform.

3) Bending Test (Intra-deployment)

A bending stent simulation evaluates the flexibility of a stent in its crimped state, measuring its ability to navigate through tortuous vascular paths during delivery.

a) Define stent

1- Import the full crimped stent geometry.
2- Define the material properties for the stent.

b) Boundary Conditions

1- Fix the two edges at the center of the stent.
2- Apply moments on both sides of the stent. (Figure 31)

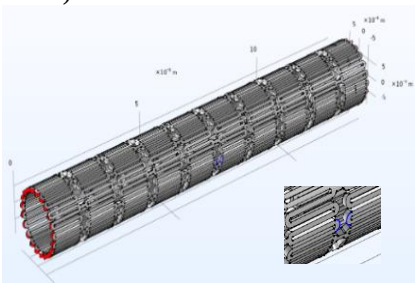

Figure 31 Boundary condition for Bending Resistance test. Red represents the apply moment and blue represents the fixed edge.

c) Meshing

Generate a high-accuracy mesh with fine control to ensure precision in simulation results

d) Simulation and Results

1- Bending resistance

Evaluate the bending resistance by plotting the moment-curvature curve and calculating the area under the curve in the linear region, which represents the stent's resistance to bending. (Figure 32).

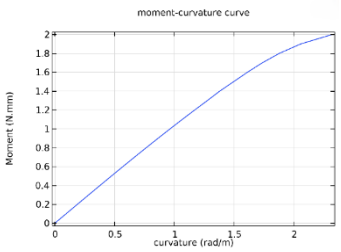

Figure 32 Moment-curvature curve.

4) Bending Fatigue

a) Define stent

1- Import the full stent geometry deployed state.
2- Define the material properties for the stent.

b) Geometry

Create rigid connectors on both sides of the stent. (Figure 33).

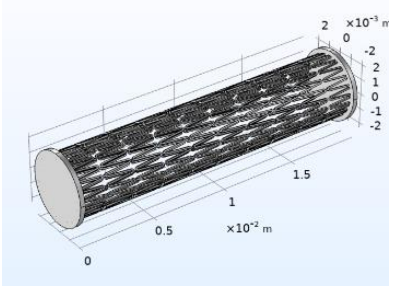

Figure 33 Stent with rigid connectors on both sides.

c) Boundary Conditions

1- Fix the left cylinder
2- Apply moments to the right cylinder of the stent.

d) Meshing

Generate a high-accuracy mesh with fine control to ensure precision in simulation results.

e) Simulation and Results

The fatigue usage factor is calculated using the Findley, Matake, and Maximum Normal Stress Criteria. (Figure 35)

The number of cycles to failure is estimated using Goodman and Soderberg Methods (Figure 34).

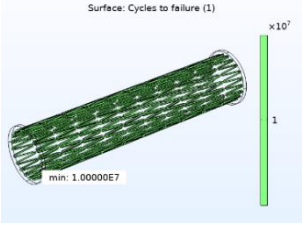

Figure 34 Distribute the failure cycles across all points for Bending Fatigue (deployed state).

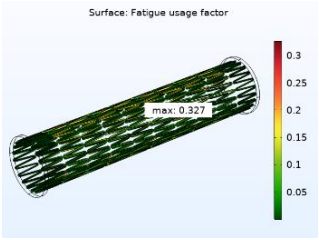

Figure 35 Distribute the usage factor.

5) Radial Fatigue

a) Define stent

1- Import the full stent geometry (unit cell deployed stent).
2- Define the material properties for the stent.

b) Boundary Conditions

1- Apply symmetry on the repeated side of the stent's unit cell (Figure 36).
2- Apply fluctuating pressure within the stent's unit cell, simulating blood pressure variations between 80-mm Hg and 120-mm Hg.

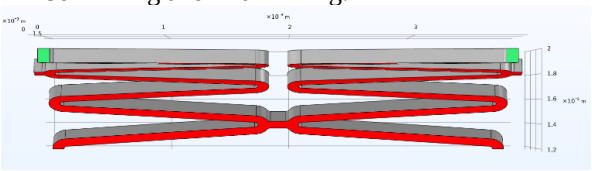

Figure 36 Applying Boundary condition. Green color represents the Symmetry condition while the Red represent the Inner Radial Pressure.

c) Meshing

Generate a high-accuracy mesh with fine control to ensure precision in simulation results.

d) Simulation and Results

Same results as bending fatigue (Figure 38).

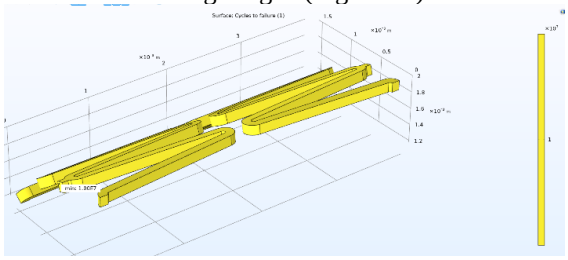

Figure 37 Distribute the failure cycles across all points for Radial Fatigue.

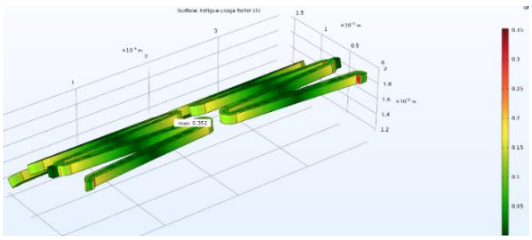

Figure 38 Distribute the usage factor across all points for Radial Fatigue.

E. Optimization

In stent design, optimization can be categorized into two types. Parametric optimization focuses on geometric parameters such as width, thickness, and length, and is performed on a continuous scale. Shape optimization, on the other hand, addresses stent configurations, including the number of connectors, number of rings, and cross-sectional shape, and is conducted on a discrete scale [4].

In our design, we have chosen to use parametric optimization, focusing on strut width and strut length as the free variables to be optimized. These parameters were selected because they significantly influence the performance outcomes, as demonstrated in study on the influence of geometric design [3].

SolidWorks® was utilized to design CAD geometries of stents with varying strut lengths and widths, maintaining a fixed number of connectors. These geometries were subsequently imported into **COMSOL®** for simulation and analysis. Due to limitations in **COMSOL®**, such as the inability to perform continuous shape or parametric optimization and the high computational cost of individual simulations, an alternative optimization strategy was developed.

This approach involved the following steps: employing Design of Experiments (DOE) to generate an initial dataset, leveraging machine learning (ML) models to predict intermediate dataset values, applying curve fitting to derive objective functions, and using a Genetic Algorithm (GA) to determine the optimized stent parameters based on the output functions. This methodology facilitated efficient optimization while addressing the constraints of simulation tools.

1) Design of Experiment

The Design of Experiment (DOE) for testing the combination of 3 strut lengths and 3 strut widths involves creating a full factorial design MiniTab® with 9 experimental runs, where each combination of strut length (short, medium, long) and strut width (narrow, medium, wide) is tested. The experiment will examine how these design parameters influence key performance metrics such as radial strength, fatigue resistance, and flexibility. The results will be analyzed to identify the optimal combination of strut length and width that meets the desired stent performance requirements. The (Figure 39) illustrates the dimensions chosen for the DOE, determined based on the minimum and maximum feasible widths and thicknesses.

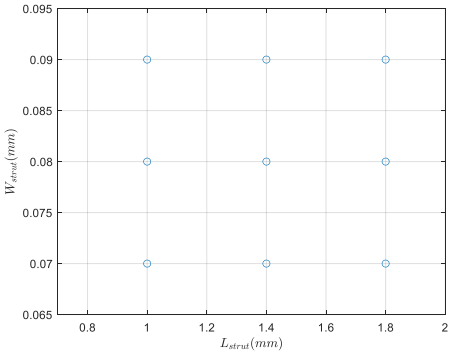

Figure 39 The nine experimental runs.

2) Machine Learning and Curve Fitting

Following the evaluation of stent performance across the 9 simulations, the outputs (KPIs) and inputs (L_{strut}, W_{strut}) were normalized, to the range [0, 1]. This normalization was performed to aid in optimization and simplify the interpretation of the results by bringing different parameters to the same scale. The normalization formula:

$$\hat{Z} = \frac{Z - Z_{min}}{Z_{max} - Z_{min}} \quad (18)$$

Where, $\hat{Z}$ and Z denote the normalized and absolute values, whilst Z_{min} and Z_{max} denote the minimum and maximum attainable values.

The machine learning tool **Orange®** was employed to estimate stent performance across additional values within the specified range of (L_{strut}, W_{strut}). This expanded dataset improves the accuracy of fitting the data to a predictive equation. The predicted data was generated by training the machine learning model, Neural Network, using the 9 tested data points obtained from **COMSOL®**. This model was then used to predict an additional 16 data points, as illustrated in (Figure 40). Subsequently, these 25 samples were fitted to equations for use in optimization.

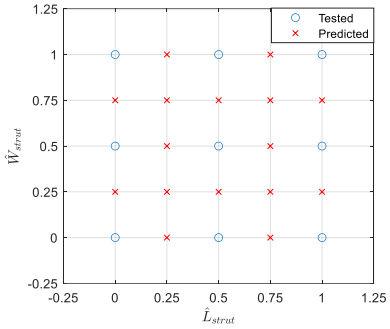

Figure 40 The total samples (normalized) after using machine learning.

The fitting equation employed is:

$$\hat{y}(\hat{L}_{strut}, \hat{W}_{strut}) = a_1 + a_2\hat{L}_{strut} + a_3\hat{W}_{strut} + a_4\hat{L}_{strut}\hat{W}_{strut} + a_5{\hat{L}_{strut}}^2 + a_6{\hat{W}_{strut}}^2 + a_7{\hat{L}_{strut}}^2\hat{W}_{strut} + a_8\hat{L}_{strut}{\hat{W}_{strut}}^2 + a_9{\hat{L}_{strut}}^3 + a_{10}{\hat{W}_{strut}}^3 \quad (19)$$

Where yˆ is the normalized output, $\hat{L}_{strut}$ *and* $\hat{W}_{strut}$ are the normalized strut length and width respectively, and the coefficients $(a_1, a_2, \dots, a_9)$ are determined using least square method. The coefficients are determined in **MATLAB®** using the backslash operator. For example, foreshortening fitting is shown in (Figure 41).

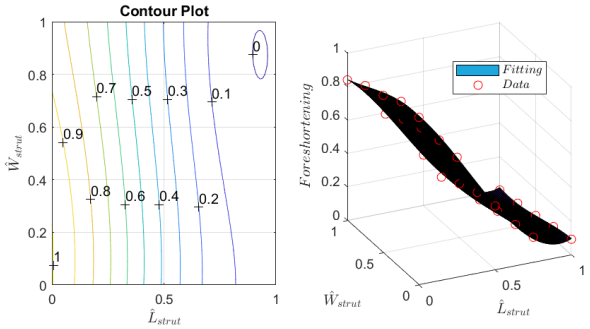

Figure 41 Foreshortening Fitting.

3) Multi-Objective Optimization

The gamultiobj function in **MATLAB®** is used for solving multi-objective optimization problems using a genetic algorithm. It is part of **MATLAB®**'s Global Optimization Toolbox and can handle problems involving multiple conflicting objectives while finding a set of optimal solutions. The multi-objective optimization problem proposed in this study was formulated as follows:

$$\begin{matrix} Dogboning\ (L_{strut}, W_{strut}) \\ Foreshortening\ (L_{strut}, W_{strut}) \\ Radial\ Recoil\ (L_{strut}, W_{strut}) \\ Maximum\ Stress\ (L_{strut}, W_{strut}) \\ Residual\ Stress\ (L_{strut}, W_{strut}) \\ -Radial\ Strength\ (L_{strut}, W_{strut}) \\ -Radial\ Stiffness\ (L_{strut}, W_{strut}) \\ Bending\ Resistance\ (L_{strut}, W_{strut}) \\ -Artery\ Coverage\ (L_{strut}, W_{strut}) \end{matrix} \quad minimize \quad , \quad subject\ to \begin{cases} 1.000\ mm \le L_{strut} \le 1.800\ mm \\ 0.070\ mm \le W_{strut} \le 0.090 mm \end{cases}$$

Note that Radial Strength, Radial Stiffness, and Artery Coverage have a minus sign because the goal here is to maximize these metrics.

The optimization of these equations involves conflicting objectives, leading to a set of possible solutions rather than a single definitive one. To address this, we applied the weighted sum method for multi-objective optimization. This approach transforms multiple objectives into a single composite objective by assigning relative importance, or "weights," to each one. By doing so, the method provides a unique solution that reflects the specified trade-offs. The method operates by normalizing the n objective functions $f_1(\boldsymbol{x}), f_2(\boldsymbol{x}), \dots, f_n(\boldsymbol{x})$ to ensure no single objective dominates due to scale differences. Each objective $f_i(\boldsymbol{x})$ is then assigned a weight w_i, where $\sum_{i=1}^{n} w_i = 1\ and\ w_i \in [0,1]$, reflecting its relative importance. These weighted objectives are combined into a single composite function $F(\boldsymbol{x}) = \sum_{i=1}^{n} w_i f_i(\boldsymbol{x})$, reducing the problem to a standard single-objective optimization task [27].

So, using this method the following problem formulation will be:

$$minimize\ F(\boldsymbol{x}), \quad subject\ to\ \boldsymbol{x} \in [0,1]^2 \quad (20)$$

where F(x) is the performance measure to be minimized and $\boldsymbol{x} = [\hat{L}_{strut}, \hat{W}_{strut}]$ is the vector of design parameters. The gamultiobj function, designed for multi-objective optimization, can also manage this single-objective formulation, providing a unique solution.

F. Cost Analysis

1) Cost Assumptions

- Prices: Based on current market rates, considering only manufacturing costs.
- Material: 316L Stainless Steel with a density of 8000 kg/m³ and a stent volume of 3.8276×10^{-9} m³. Material cost per stent is $0.000236 at $7.695/kg.
- Manufacturing Costs:
  - Laser Cutting: $400/hour
  - 3D Printing: $300/hour
  - Braiding: $20/hour
  - Micro-Injection Molding: $100/hour + $5,000 fixed mold cost.

2) Cost Calculations

- Manufacturing Costs:
  - Laser Cutting: 14 minutes per stent, cost: $93.33.
  - 3D Printing: 20 minutes per stent, cost: $100.14.
  - Braiding Technique: 30 minutes per stent, cost: $10.24.
  - Micro-Injection Molding: 25 minutes per stent, fixed mold cost of $50 per stent, total cost: $70.24.

3) Sensitivity Analysis

Table 5 Sensitivity Analysis.

Manufacturing Method	Base Cost (USD)	+10% (USD)	+15% (USD)	+20% (USD)
Laser Cutting	$93.33	$102.66	$107.332	$111.999
3D Printing	$100.136	$110.149	$115.156	$120.163
Braiding Technique	$10.236	$11.260	$11.771	$12.283
Micro-Injection Molding	$70.236	$77.259	$80.271	$84.283

4) Comparative Analysis: Optimized Stent Design vs. Commercial Stents

Table 6 Comparative Analysis.

Feature	Optimized Stent	Abbott XIENCE Sierra	Boston Scientific Promus PREMIER
Material	316L Stainless Steel + Drug Coating	Cobalt-Chromium Alloy + Drug Coating	Platinum-Chromium Alloy + Drug Coating
Coating	Yes	Yes	Yes
Radial Strength (N/mm)	11.39	12.00	11.50
Recoil (mm)	0.01463	0.015	0.015
Maximum Stress (MPa)	429	450	460
Residual Stress (MPa)	275	280	290
Average Cost (USD)	$111.999 (including 20 %profit)	$250–$300	$300–$350
Manufacturing Method	Laser Cutting	Laser Cutting	Laser Cutting

Justification for Choosing the Optimized Stent Design

- Cost-Effectiveness:

Our stent is manufactured at $111.999 per unit (Table 6) significantly lower than commercial alternatives ($250–$350) (Table 6).

- Mechanical Performance:

Competitive radial strength (11.39 N/mm) and minimal recoil (0.01463 mm), ensuring reliable deployment.

- Material and Coating:

316L Stainless Steel offers superior corrosion resistance and biocompatibility, combined with a drug coating for enhanced therapeutic benefits.

IV. Results and Discussion

The discussion is based on models that applied simulation tests to assess their performance. The next table (Table 7) shows the main results in the project.

Table 7 The main results.

Outputs	Literature Range	Simulations Range	Optimum Model	Predicted Values for the Optimum
Dogboning	0.015 - 0.15	0.0216 - 0.0402	0.0272	0.0257
Foreshortening	0.001 - 0.05	0.0040 - 0.0140	0.0046	0.0042
Radial Recoil	0.0145 - 0.043	0.0130 - 0.0147	0.014631	0.013106
Maximum Stress (MPa)	-	357 - 553	429.000000	417.415525
Residual Stress (MPa)	-	280 - 387	275.000000	295.454271
Radial Strength (N/mm)	0.06 – 0.63	0.0627 - 0.2467	0.079746	0.096358
Radial Stiffness (N/mm^2)	-	7.3699 - 91.9097	14.758007	8.591048
Bending Resistance (N)	0.0001 - 0.004	0.000044 - 0.001335	0.000188	0.000068
Artery Coverage (%)	12 - 35	20.976 - 27.821	26.705553	26.551643
Fatigue (Usage Factor)	<1	-	0.458	-

The simulation results showcase the effectiveness of the optimized stent design, aligning closely with literature values and confirming its exceptional mechanical performance. Metrics like dogboning (0.0216–0.0402) and foreshortening (0.0040–0.0140) not only fall within accepted ranges but also highlight the design's precision and adaptability during deployment. Radial recoil (0.0130–0.0147) mirrors the literature values, ensuring consistent lumen support post-expansion. Importantly, the maximum stress (357–553 MPa) remains well below the tensile strength threshold of 560 MPa, indicating a robust and reliable structure capable of withstanding physiological pressures. Furthermore, radial strength and stiffness demonstrate the stent's ability to provide optimal support under compression, reinforcing its mechanical excellence.

The predicted values derived from machine learning models show strong alignment with optimum simulation results, bolstering confidence in the optimization methodology. Fatigue analysis revealed a usage factor of 0.458, confirming durability under cyclical loads. The optimum strut length of 1.668 mm and width of 0.090 mm achieve ideal geometry for flexibility and support. Artery coverage of 26.705% ensures sufficient vascular support while maintaining durability. These outcomes highlight the project's success in delivering a stent design that balances clinical effectiveness, mechanical reliability, and long-term durability.

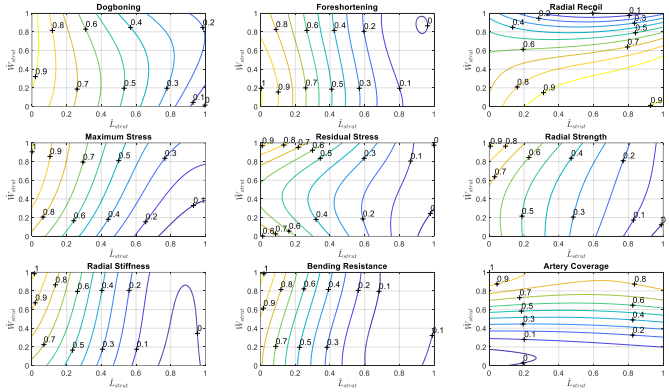

Figure 42 Contour plot from the outputs.

The results (Figure 42) clearly indicate that the length of the strut has a significant impact on various output parameters, particularly maximum stress, foreshortening, and bending resistance, increasing strut length effectively minimizes these factors. In contrast, strut width primarily influences radial recoil and artery coverage. However, the width has little effect on other outputs except for residual stress and maximum stress.

It is clear from observation that during the expansion (deployment) process, the maximum stress occurs at the inner crown radius due to stress concentration caused by the sharp curvature. The area of the deployed stent changes negligibly from its crimped state because the deployment process primarily affects the stent through bending of the struts, rather than tension. Bending results in minimal lateral deformation.

V. Conclusion and Future Work

The results of this study highlight the success of our stent design in meeting critical clinical requirements. The radial strength of 429 N/mm and radial stiffness of 14.58 N/mm confirm the stent's ability to maintain vessel patency under physiological pressures while preserving flexibility for deployment in complex anatomies. The artery coverage of 26.56% ensures effective restoration of blood flow, closely matching the diameter of a healthy artery. Additionally, the fatigue analysis, with a usage factor of 0.458, indicates high

durability and reliability for long-term use under repetitive loading conditions.

This project addressed the inherent challenges of optimizing conflicting objectives, such as balancing radial strength, flexibility, and fatigue resistance. By applying a weighted optimization approach, we carefully navigated these trade-offs to achieve a design that excels in multiple performance metrics. These results not only validate the effectiveness of our optimization strategy but also highlight the potential of our methodology to contribute to the development of advanced, reliable, and clinically relevant coronary stents.

Future Work

For future stent designs, simulations include artery-stent and blood flow interactions, hemodynamic performance, radial strength with residual stress, collapse pressure, malposition tests, connector design, drug release analysis, and simulations for other materials to optimize performance and clinical outcomes.

ACKNOWLEDGMENT

We want to thank Dr. Raguraman Kannan, our supervisor, for his constant guidance and support throughout this project. His encouragement and availability at any time motivated us to keep going, even during difficult moments. Dr. Raguraman Kannan knowledge and advice helped us stay on track and complete this work successfully.

We are also deeply thankful to our Families for their endless love and support. They stood by us through this challenging time, understanding the long hours we spent on the project. Their encouragement kept us going, especially when things felt overwhelming.

We extend our thanks to our Friends and Colleagues, who shared this journey with us, offering encouragement and support when we needed it most. Their presence made this experience more enjoyable and meaningful.

Lastly, we are grateful to our University, Professors, and Doctors for giving us the opportunity to grow and learn over the past years. As we graduate, we will cherish the moments and experiences we had in this department, which helped shape our future.

Thank you all for being a part of this journey.

REFERENCES

1. *Angioplasty and Stent Procedures*. Available from: https://www.azuravasculcarcare.com/medical-services/dialysis-access-management/angioplasty-stent-procedures/.
2. Budynas, R.G. and J.K. Nisbett, *Shigley's Mechanical Engineering Design*. 2020: McGraw-Hill Education.
3. Ribeiro, N.S., J. Folgado, and H.C. Rodrigues, *Surrogate-based visualization and sensitivity analysis of coronary stent performance: A study on the influence of geometric design.* International Journal for Numerical Methods in Biomedical Engineering, 2018. **34**(10): p. e3125.
4. Kapoor, A., et al., *The road to the ideal stent: A review of stent design optimisation methods, findings, and opportunities.* Materials & Design, 2024. **237**: p. 112556.
5. Pan, C., Y. Han, and J. Lu, *Structural Design of Vascular Stents: A Review*. Micromachines, 2021. **12**(7): p. 770.
6. Shah, D.A.R. *Coronary Stent Design: The Backbone of Interventional Cardiology*. 2016 [cited 2024; Available from: https://youtu.be/tzNVf1zzl4M?si=cti4hxzATkWM4dTq.
7. Buccheri, D., et al., *Understanding and managing in-stent restenosis: a review of clinical data, from pathogenesis to treatment.* J Thorac Dis, 2016. **8**(10): p. E1150-e1162.
8. Team, H.E. *What Is Restenosis?* 2019 [cited 2024; Available from: https://www.healthline.com/health/restenosis#symptoms.
9. Souteyrand, G., et al., *Mechanisms of stent thrombosis analysed by optical coherence tomography: insights from the national PESTO French registry*. European Heart Journal, 2016. **37**(15): p. 1208-1216.
10. Torii, S., et al., *Drug-eluting coronary stents: insights from preclinical and pathology studies.* Nature Reviews Cardiology, 2020. **17**(1): p. 37-51.
11. Fam, J.M., et al., *Conformability in everolimus-eluting bioresorbable scaffolds compared with metal platform coronary stents in long lesions.* Int J Cardiovasc Imaging, 2017. **33**(12): p. 1863-1871.
12. Food, U. and D. Administration, *Non-clinical engineering tests and recommended labeling for intravascular stents and associated delivery systems.* US Food and Drug Administration: Rockville, MD, USA, 2010.
13. Ribeiro, N.S., J. Folgado, and H.C. Rodrigues, *Surrogate-based multi-objective design optimization of a coronary stent: Altering geometry toward improved biomechanical performance.* International Journal for Numerical Methods in Biomedical Engineering, 2021. **37**(6): p. e3453.
14. Materials, A.S.f.T., *Standard Test Method for Measuring Intrinsic Elastic Recoil of Balloon-Expandable Stents: Designation: F2079-09(Reapproved 2013)*. 2013: ASTM.
15. Materials, A.S.f.T., *Standard Guide for Three-Point Bending of Balloon-Expandable Vascular Stents and Stent Systems. Designation: F2606 − 08 (Reapproved 2021)*. 2021: ASTM.
16. Wiesent, L., et al., *Experimentally validated simulation of coronary stents considering different dogboning ratios and asymmetric stent positioning.* PLOS ONE, 2019. **14**(10): p. e0224026.
17. Blair, R., et al., *Multi-objective optimisation of material properties and strut geometry for poly(L-lactic acid) coronary stents using response surface methodology.* PLOS ONE, 2019. **14**: p. e0218768.
18. *Fatigue Module User's Guide.*
19. COMSOL, *Fatigue Module Application Library Manual.*
20. Jiang, W., et al., *A Review on Manufacturing and Post-Processing Technology of Vascular Stents.* Micromachines (Basel), 2022. **13**(1).
21. Polanec, B., J. Kramberger, and S. Glodež, *A review of production technologies and materials for manufacturing of cardiovascular stents.* Advances in Production Engineering & Management, 2020. **15**: p. 390-402.
22. Russell, R.S. and B.W. Taylor, *Operations and Supply Chain Management*. 2019: Wiley.
23. Ashby, M.F., *Materials Selection in Mechanical Design*. 2010: Butterworth-Heinemann.
24. Emonde, C.K., et al., *Radiopacity Enhancements in Polymeric Implant Biomaterials: A Comprehensive Literature Review.* ACS Biomater Sci Eng, 2024. **10**(3): p. 1323-1334.
25. Selector, A.G. *Smarter Materials Choices*. [cited 2024; Available from: https://www.ansys.com/products/materials/granta-selector.

26. COMSOL. *Simulate real-world designs, devices, and processes with multiphysics software from COMSOL*. Available from: https://www.comsol.com/.

27. Marler, R. and J. Arora, *The weighted sum method for multi-objective optimization: New insights.* Structural and Multidisciplinary Optimization, 2010. **41**: p. 853-862.

28. Granta, A. *Getting Started with Granta Selector*. 2022; Available from: https://youtube.com/playlist?list=PLm2iroHj73L9ZLFKpquLSbB9k4ZViTCZP&si=YWWfrJyh3nU3poWi.